

# Strategic Investment in Energy Markets: A Multiparametric Programming Approach

Sina Taheri *Student Member, IEEE*, Vassilis Kekatos, *Senior Member, IEEE*, and Harsha Veeramachaneni

**Abstract**—An investor has to carefully select the location and size of new generation units it intends to build, since adding capacity in a market affects the profit from units this investor may already own. To capture this closed-loop characteristic, strategic investment (SI) can be posed as a bilevel optimization. By analytically studying a small market, we first show that its objective function can be non-convex and discontinuous. Realizing that existing mixed-integer problem formulations become impractical for larger markets and increasing number of scenarios, this work put forth two SI solvers: a grid search to handle setups where the candidate investment locations are few, and a stochastic gradient descent approach for otherwise. Both solvers leverage the powerful toolbox of multiparametric programming (MPP), each in a unique way. The grid search entails finding the primal/dual solutions for a large number of optimal power flow (OPF) problems, which nonetheless can be efficiently computed several at once thanks to the properties of MPP. The same properties facilitate the rapid calculation of gradients in a mini-batch fashion, thus accelerating the implementation of a stochastic gradient descent search. Tests on the IEEE 118-bus system using real-world data corroborate the advantages of the novel MPP-aided solvers.

**Index Terms**—Mathematical programming with equilibrium constraints; bilevel programming; locational marginal prices.

## I. INTRODUCTION

Suppose an investor intends to build one or more power plants with which it will be participating in an electricity market. The investor may already own generation units bidding in the same market. By adding generation capacity and depending on transmission congestion and load demand, electricity prices and generation schedules may be altered in a way so that its total financial gain from existing as well as new units is lowered. The goal of the investor is to find the optimal location and size of the new generation units to maximize its total profit. This task of *strategic investment (SI)* is challenging for three reasons. First, the variables involved in SI, namely the generation schedules and electricity prices, are not known beforehand but are computed as the solutions of an optimization problem, a linearized optimal power flow (OPF). Second, an investment can change the market outcome (prices and generation schedules), rendering SI a complex closed-loop problem. Third, increasing uncertainties introduced by renewable generation, loads, fuel prices, and bids from rival generators, call for stochastic methods thus further increasing the complexity of SI.

A promising method to handle the closed-loop complication of the SI task is posing it as a bi-level optimization [1]. The inner level involves the OPF that clears the market and decides generation schedules and prices given generation capacities. The outer level aims to maximize the market profit for dispatching new and existing units minus the investment cost for the new units. Nonetheless, this bi-level formulation calls for complex complementarity methods [2]; see [3] for a

comprehensive survey. In the case of market OPFs with linear constraints, complementarity methods convert the bi-level problem into a single-level optimization upon replacing the inner problem with its Karush-Kuhn-Tucker (KKT) conditions. While complementarity methods promise globally optimal investment decisions, they entail computationally prohibitive mixed-integer programs. Such models may not scale gracefully in large power networks and take into account a sufficient number of uncertain market scenarios. Alternatively, works like [4], [5], [6] use scenario-based consensus alternating direction method of multipliers or progressive hedging to decompose the related mixed-integer programs, yet at the expense of losing global optimality.

The complexity of complementarity models prompted us to waive the need for bi-level programming. The SI task could be dealt with by solving the OPF clearing the market for each possible combination of scenario and investment option. However, this process is also challenging due to the sheer number of OPFs that need to be solved, calling for efficient OPF solvers for a large number of market scenarios. Interestingly, the OPF problem under the linearized grid model, the so-called DC-OPF, can be viewed as an instance of multiparametric programming (MPP), where loads, generation capacities, and bids are considered as its parameters. As explained in Section IV, under certain conditions, the MPP toolbox can partition the parameter space into polytopes termed *critical regions* for which the primal and dual solutions can be identified as affine functions of the problem parameters [7], [8]. The boundaries of these regions as well as the associated affine functions depend on which constraints are active at optimality, and hence, the DC-OPF needs to be solved only once per critical region. This latter property facilitates solving a large number of DC-OPFs with relatively small computational burden.

MPP has appeared before in power systems operations. The notion of congestion patterns in energy markets identified by [9] pertains exactly to the critical regions of MPP. The same regions also give rise to the active sets learned in [10], [11]. Reference [12] combine MPP with importance sampling over critical regions to compute the probability distribution of locational marginal prices (LMPs). The polytopic description of critical regions allows [13] to train a support vector machine classifier and estimate LMPs given loads. In the context of distribution grids, reference [14] leverages MPP to handle efficiently a large number of distribution OPF instances, and thus expedite probabilistic hosting capacity analysis. However, none of the previous works engages MPP to deal with the complex bilevel setup involved in SI.

The contributions of this work is fourfold: *c1)* Study SI analytically for a simple power network to demonstrate the challenges involved; *c2)* Extend existing MPP claims to the OPF problem used to clear electricity markets; *c3)* Develop

an algorithm to compute efficiently the primal/dual outcomes of hundreds of OPF instances at a time. The algorithm can accelerate by an order of magnitude a brute-force grid search to cope with the SI task when the number of investment locations and scenarios are relatively small; and *c4*) Devise a stochastic gradient descent (SGD) scheme to address directly the outer layer of the SI task, especially when multiple investment locations are considered. By uniquely exploiting MPP properties, this SGD scheme calculates gradients in a highly scalable mini-batch fashion.

## II. STRATEGIC INVESTMENT IN ELECTRICITY MARKETS

### A. Modeling Electricity Markets

Day-ahead energy markets are commonly modeled using the so termed DC grid model, which is briefly reviewed next. Suppose the energy market operates over a system with  $N$  buses and  $L$  transmission lines. Its topology is captured by the  $L \times N$  branch-bus incidence matrix  $\tilde{\mathbf{A}}$ . To express line flows in terms of power injections, let  $x_j$  be the reactance of line  $j$  and  $\mathbf{X}$  be an  $L \times L$  diagonal matrix having  $x_j^{-1}$ 's as its diagonal entries. Under the assumption of a lossless grid, as long as  $\mathbf{p}^\top \mathbf{1} = 0$ , line flows relate to bus injections as  $\mathbf{f} = \mathbf{S}\mathbf{p}$ , where  $\mathbf{S}$  is the power-transfer distribution factor (PTDF) matrix defined as  $\mathbf{S} := [\mathbf{0} \ \mathbf{X}\tilde{\mathbf{A}}\tilde{\mathbf{A}}^\top\mathbf{X}^{-1}]$ ;  $\tilde{\mathbf{A}}$  is the *reduced* branch-incidence matrix obtained from  $\tilde{\mathbf{A}}$  upon removing its first column; and  $\mathbf{\Gamma} := \tilde{\mathbf{A}}^\top \mathbf{X} \tilde{\mathbf{A}} \succ 0$  is the reduced bus reactance matrix; see e.g., [15] for details.

In an energy market, the independent system operator (ISO) calculates the generation schedule and electricity prices upon solving a linear or quadratic program to minimize the total generation cost subject to power balance and line flow constraints. From the viewpoint of a strategic investor, one can identify three types of generators in a market [2]: existing units owned by rival entities; existing units owned by the investor; and new units under investment. The power schedules corresponding to these units are denoted respectively by  $(\mathbf{p}_r, \mathbf{p}_e, \mathbf{p}_n)$ . For notational brevity, suppose all unit types exist at all buses with possibly zero capacities. The market is cleared by the DC-OPF

$$\min_{\mathbf{p}_r, \mathbf{p}_e, \mathbf{p}_n} f_r(\mathbf{p}_r) + f_e(\mathbf{p}_e) + f_n(\mathbf{p}_n) \quad (1a)$$

$$\text{s.to } \mathbf{1}^\top (\mathbf{p}_r + \mathbf{p}_e + \mathbf{p}_n - \boldsymbol{\ell}) = 0 \quad : \lambda_0 \quad (1b)$$

$$-\bar{\mathbf{f}} \leq \mathbf{S}(\mathbf{p}_r + \mathbf{p}_e + \mathbf{p}_n - \boldsymbol{\ell}) \leq \bar{\mathbf{f}} \quad : \underline{\boldsymbol{\mu}}, \bar{\boldsymbol{\mu}} \quad (1c)$$

$$\mathbf{0} \leq \mathbf{p}_r \leq \bar{\mathbf{p}}_r \quad : \underline{\boldsymbol{\gamma}}_r, \bar{\boldsymbol{\gamma}}_r \quad (1d)$$

$$\mathbf{0} \leq \mathbf{p}_e \leq \bar{\mathbf{p}}_e \quad : \underline{\boldsymbol{\gamma}}_e, \bar{\boldsymbol{\gamma}}_e \quad (1e)$$

$$\mathbf{0} \leq \mathbf{p}_n \leq \bar{\mathbf{p}}_n \quad : \underline{\boldsymbol{\gamma}}_n, \bar{\boldsymbol{\gamma}}_n. \quad (1f)$$

Function  $f_r(\mathbf{p}_r) = \frac{1}{2} \mathbf{p}_r^\top \mathbf{H}_r \mathbf{p}_r + \mathbf{c}_r^\top \mathbf{p}_r$  models the generation cost for rival units. The diagonal matrix  $\mathbf{H}_r$  and vector  $\mathbf{c}_r$  contain positive values [16]. The generation costs for existing and new units  $f_e$  and  $f_n$  are defined similarly. Constraint (1b) ensures power balance. Constraint (1c) enforces given line flow limits  $\bar{\mathbf{f}}$ . Constraints (1e)–(1d) impose capacity limits  $(\bar{\mathbf{p}}_r, \bar{\mathbf{p}}_e, \bar{\mathbf{p}}_n)$  on generation schedules. Dual variables are shown in the right-hand side of the constraints in (1). To account for renewable generation, vector  $\bar{\mathbf{p}}_r$  is the available

capacity of the rival units, and can be modeled as  $\bar{\mathbf{p}}_r = \boldsymbol{\alpha}_r \odot \hat{\mathbf{p}}_r$  with  $\odot$  denoting the entry-wise multiplication and  $\hat{\mathbf{p}}_r$  being the maximum (installed) capacity that is a constant. The scalar  $\alpha_{i,r}$  is the capacity factor for unit  $i$ . For conventional units (e.g., coal plants), we have  $\alpha_{i,r} = 1$ . For renewable units, the capacity  $\alpha_{i,r} \leq 1$  changes with time to capture the available wind energy as a percentage of the maximum capacity. Similarly define  $(\boldsymbol{\alpha}_e, \boldsymbol{\alpha}_n, \hat{\mathbf{p}}_e)$  and denote the maximum capacity of new units by vector  $\mathbf{x}$ , which is what the market participant would like to invest on.

The ISO solves (1) for every hour to find the optimal schedules  $(\mathbf{p}_r, \mathbf{p}_e, \mathbf{p}_n)$  and LMPs computed as

$$\boldsymbol{\pi} = -\lambda_0 \mathbf{1} + \mathbf{S}^\top (\underline{\boldsymbol{\mu}} - \bar{\boldsymbol{\mu}}). \quad (2)$$

Here we have slightly abused notation and used the same symbols with (1) to denote also the optimal primal and dual variables of the problem. The first summand in the RHS of (2) denotes the marginal energy component (MEC) and the second one the marginal congestion component (MCC). LMPs also have also a marginal loss component (MLC) to account for network losses, but is generally small and is ignored here. The next section presents the strategic investment task upon adapting the formulation of [2].

### B. Problem Formulation

Strategic investment in electricity markets can be viewed as a minimization problem where the cost is the amortized cost for investing in the new units minus the expected revenue obtained from the market through the new units and the existing own units. The investment cost is generally a known linear function  $\mathbf{k}^\top \mathbf{x}$  of the generation capacity. The revenue is made up by the payment received from the ISO (generation schedule times LMP) minus the true generation cost

$$f(\mathbf{x}) := \mathbf{k}^\top \mathbf{x} - \mathbb{E} [\boldsymbol{\pi}^\top (\mathbf{p}_e + \mathbf{p}_n) - g_e(\mathbf{p}_e) - g_n(\mathbf{p}_n)]. \quad (3)$$

Note  $f$  involves the actual cost of generation  $g_e(\mathbf{p}_e) + g_n(\mathbf{p}_n)$  rather than the bid  $f_e(\mathbf{p}_e) + f_n(\mathbf{p}_n)$  submitted to the market. This is because the latter can be sometimes larger than the former for some or all  $(\mathbf{p}_e, \mathbf{p}_n)$  [2]. The expectation in (3) is applied over all uncertainties, such as the demand vector  $\boldsymbol{\ell}$  or possible changes in unit capacities  $(\bar{\mathbf{p}}_e, \bar{\mathbf{p}}_r)$  and bids.

The task of strategic investment can be now stated as

$$\min_{\mathbf{x} \in \mathcal{X}} f(\mathbf{x}) \quad (4a)$$

$$\text{s.to } \{\boldsymbol{\pi}, \mathbf{p}_e, \mathbf{p}_n\} \text{ being solutions of (1).} \quad (4b)$$

The set  $\mathcal{X} := \{\mathbf{x} : \underline{\mathbf{x}} \leq \mathbf{x} \leq \bar{\mathbf{x}}, \mathbf{\Delta} \mathbf{x} \leq \boldsymbol{\delta}\}$  captures limits on investment options. The constraint  $\mathbf{\Delta} \mathbf{x} \leq \boldsymbol{\delta}$  in particular could model an upper bound on the total MW capacity installed or the total number of wind turbines purchased. Investments  $\mathbf{x}$  may also be restricted to take discrete values. As in [2], we further postulate two assumptions on the problem setup.

**Assumption 1.** *The transmission network topology captured by  $(\mathbf{S}, \bar{\mathbf{f}})$  is known and remains constant.*

**Assumption 2.** *Problem parameters  $(\boldsymbol{\ell}, \bar{\mathbf{p}}_r, \bar{\mathbf{p}}_e, \bar{\mathbf{f}})$  are such that the DC-OPF of (1) is feasible for all  $\mathbf{x} \in \mathcal{X}$ .*

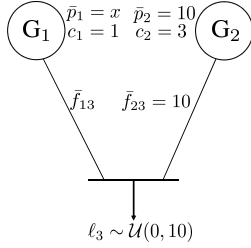


Fig. 1. A simple 3-bus power system showcasing the challenges in solving (4).

According to Assumption 2, the power system can be dispatched without the new units. Even under these assumptions, problem (4) is challenging due to three reasons: *i*) Constraint (4b) is an optimization problem itself; *ii*) The products between primal and dual variables under the expectation of (3) are non-convex; and *iii*) Evaluating the expectation in  $f(\mathbf{x})$  may be prohibitive. The investment task of (4) will be termed as the *outer problem* and the DC-OPF of (1) given  $\mathbf{x}$  as the *inner problem*. SI can be challenging even in a small system as elucidated next.

### C. An Illustrative 3-bus Example

Consider the 3-bus power system of Fig. 1. An investor considers building a generator on bus 1. A rival generator is located at bus 2 having capacity  $\bar{p}_2 = 10$  pu. Bus 3 hosts a load  $\ell_3$  whose value is modeled as a random variable uniformly distributed within  $(0, 10)$ . The limit for line  $b = (2, 3)$  is  $\bar{f}_b = 10$ , while the limit  $\bar{f}_a$  for line  $a = (1, 3)$  is left as a variable to study its effect on strategic investment. Apparently, the DC-OPF problem is always feasible.

For this setup, there is no existing own generator, so  $f_e = g_e = 0$ . Let us assume linear bidding functions  $f_n(\mathbf{p}_n) = c_1 p_1$  and  $f_r(\mathbf{p}_r) = c_2 p_2$  with  $c_1 = 1$  and  $c_2 = 3$ . Due to the simplicity of the problem, its optimal primal/dual pairs can be readily computed upon enumerating all possible orderings for the triplet  $\{x_1, \ell_3, \bar{f}_a\}$ . In detail, if  $x_1 \leq \bar{f}_a$ , we get that

$$(p_1, \pi_1) = \begin{cases} (\ell_3, 1), & \ell_3 \leq x_1 \leq \bar{f}_a \\ (x_1, 3), & x_1 < \ell_3 \leq \bar{f}_a \text{ or } x_1 < \bar{f}_a < \ell_3. \end{cases}$$

If on the other hand  $x_1 > \bar{f}_a$ , we get that

$$(p_1, \pi_1) = \begin{cases} (\ell_3, 1), & \ell_3 \leq \bar{f}_a < x_1 \\ (\bar{f}_a, 1), & \bar{f}_a < \ell_3 < x_1 \text{ or } \bar{f}_a < x_1 < \ell_3. \end{cases}$$

Given the aforesaid cases and that  $\ell_3$  is uniformly distributed, the expectation in (4a) can be evaluated as

$$\mathbb{E}[\pi_1 p_1] = \int_0^{x_1} \frac{\ell_3}{10} d\ell_3 + \int_{x_1}^{10} \frac{3x_1}{10} d\ell_3 = 3x_1 - \frac{x_1^2}{4}, x_1 \leq \bar{f}_a$$

$$\mathbb{E}[\pi_1 p_1] = \int_0^{\bar{f}_a} \frac{\ell_3}{10} d\ell_3 + \int_{\bar{f}_a}^{10} \frac{\bar{f}_a}{10} d\ell_3 = \bar{f}_a - \frac{\bar{f}_a^2}{20}, x_1 > \bar{f}_a$$

Without loss of generality, suppose also that  $k_1 = 0$  and  $g_n(\mathbf{p}_n) = 0$ . Then, the investment cost of (4) becomes

$$f(x_1) = \begin{cases} \frac{x_1^2}{4} - 3x_1, & x_1 \leq \bar{f}_a \\ \frac{\bar{f}_a^2}{20} - \bar{f}_a, & x_1 > \bar{f}_a. \end{cases} \quad (5)$$

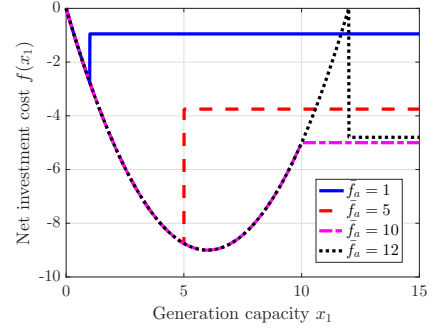


Fig. 2. The net investment cost  $f(x_1)$  for building generator 1 in the power system of Figure 1 over the capacity range of  $x_1 \in [0, 15]$  and for different capacities  $\bar{f}_a$  of line  $a = (1, 3)$ .

The interesting observation here is that  $f(x_1)$  is constant for  $x_1 > \bar{f}_a$ , and convex quadratic otherwise. This suggests that depending on the value of  $\bar{f}_a$ , the cost of (4) can be discontinuous. For the function to be continuous, we need

$$\lim_{x_1 \rightarrow \bar{f}_a^+} \left( \frac{x_1^2}{4} - 3x_1 \right) = \frac{\bar{f}_a^2}{20} - \bar{f}_a$$

which holds only for  $\bar{f}_a = 10$ . This demonstrates that SI can have a non-convex non-smooth cost. We next review the one possible method for handling the bi-level investment problem and explore its applications and limitations.

### III. MATHEMATICAL PROGRAMMING WITH EQUILIBRIUM CONSTRAINTS

Mathematical programming with equilibrium constraints (MPEC) is widely used in economics, where decisions taken by an investor affect the outcome of a market. MPEC results at bilevel optimization problems, such as the one in (4). Reference [2] posed (4) as an MPEC. For later reference, we briefly review this approach, which proceeds in three steps.

First, the bilinear term  $\boldsymbol{\pi}^\top(\mathbf{p}_e + \mathbf{p}_n)$  in (3) is replaced by a linear function of the primal/dual variables of the inner problem as [2]

$$\boldsymbol{\pi}^\top(\mathbf{p}_e + \mathbf{p}_n) = \mathbf{c}_r^\top \mathbf{p}_r + (\bar{\boldsymbol{\mu}} + \boldsymbol{\mu})^\top \bar{\mathbf{f}} + \bar{\boldsymbol{\gamma}}_r^\top \bar{\mathbf{p}}_r + (\bar{\boldsymbol{\mu}} - \boldsymbol{\mu})^\top \mathbf{S}\boldsymbol{\ell} + \lambda_0 \mathbf{1}^\top \boldsymbol{\ell}. \quad (6)$$

This follows from the strong duality of the inner problem and after some algebraic manipulations [2].

Secondly, the expectation in (3) is surrogated by a sample average computed over  $T$  scenarios indexed by  $t$  as

$$\hat{f}(\mathbf{x}) = \mathbf{k}^\top \mathbf{x} - \frac{1}{T} \sum_{t=1}^T [\boldsymbol{\pi}_t^\top(\mathbf{p}_{e,t} + \mathbf{p}_{n,t}) - g_e(\mathbf{p}_{e,t}) - g_n(\mathbf{p}_{n,t})]$$

so the strategic investment can be approximated as

$$\begin{aligned} \min_{\mathbf{x} \in \mathcal{X}} \hat{f}(\mathbf{x}) \\ \text{s.t. } \{\boldsymbol{\pi}, \mathbf{p}_{e,t}, \mathbf{p}_{n,t}\} \text{ being solutions of (1) for } t = 1 : T \end{aligned} \quad (7)$$

The third step replaces constraint (4b) by the KKT conditions for the inner problem. Out of the KKT conditions, primal/dual feasibility and Lagrangian optimality yield a set of linear equality and inequality constraints on the primal/dual

variables of the inner problem. Complementary slackness conditions on the other hand involve products between primal and dual variables. The latter conditions are non-convex, but can be posed using the so-termed big-M method [2]. Consider for instance the constraint  $x \geq 0$  and its related Lagrange multiplier  $\lambda \geq 0$ . The complementary slackness condition  $x \cdot \lambda = 0$  can be captured by constraints

$$0 \leq x \leq \phi M \quad 0 \leq \lambda \leq (1 - \phi)M \quad (8)$$

where  $M$  is a large constant and  $\phi$  is an auxiliary binary variable. A set of constraints similar to (8) has to be enforced for each constraint of the inner problem and every market scenario  $t$ . Following the aforesaid three steps, the bilevel problem in (4) can be reformulated as a mixed-integer linear or quadratic program (MILP/MIQP), depending on whether functions  $\{f_r, f_e, f_n, g_e, g_n\}$  are linear or quadratic.

The MPEC method of [2] finds the global minimum of (4) after approximating the expectation with scenarios. Nonetheless, the resultant mixed-integer formulation may not scale favorably for a large number of scenarios  $T$  or a large number of primal/dual variables. Moreover, finding proper values for  $M$  is challenging, since it is hard to upper bound dual variables *a priori*. To avoid computationally taxing mixed-integer formulations, we develop solvers of (4) that engage the powerful tool of MPP. The next section adapts the general MPP results to the problem structure at hand.

#### IV. MULTIPARAMETRIC PROGRAMMING (MPP)

MPP is a tool for characterizing the solutions of optimization problems dependent on a parameter vector [7]. The main idea of using MPP for SI is to handle the inner problem in (4) as an MPP with the SI vector  $\mathbf{x}$  as its parameter. To this end, consider a minimization dependent on parameter  $\boldsymbol{\theta}$  as

$$\min_{\mathbf{p}} \frac{1}{2} \mathbf{p}^\top \mathbf{H} \mathbf{p} + (\mathbf{C} \boldsymbol{\theta} + \mathbf{d})^\top \mathbf{p} \quad (9a)$$

$$\text{s.to } \mathbf{A} \mathbf{p} \leq \mathbf{E} \boldsymbol{\theta} + \mathbf{b} \quad : \boldsymbol{\lambda} \quad (9b)$$

$$\mathbf{B} \mathbf{p} = \mathbf{F} \boldsymbol{\theta} + \mathbf{y} \quad : \boldsymbol{\mu}. \quad (9c)$$

If  $\mathbf{H} = \mathbf{0}$ , problem (9) is a multiparametric linear program (MPLP). If  $\mathbf{H} \succeq \mathbf{0}$ , problem (9) is a multiparametric convex quadratic program (MPQP).

Let  $\Theta$  be the set of all  $\boldsymbol{\theta}$ 's for which (9) is feasible. According to the MPP theory [7], set  $\Theta$  can be partitioned into distinct regions, termed *critical regions*, with three interesting properties: *p1*) Each region is described as a polytope in  $\Theta$ ; *p2*) Within each region, the same subset of inequality constraints become *active*, i.e., are satisfied with equality; and *p3*) Within each region, the primal/dual solutions of (9) can be expressed as affine functions of  $\boldsymbol{\theta}$ . To elaborate on these properties, consider the Lagrangian function related to (9)

$$\mathcal{L}(\mathbf{p}; \boldsymbol{\lambda}, \boldsymbol{\mu}) = \frac{1}{2} \mathbf{p}^\top \mathbf{H} \mathbf{p} + (\mathbf{C} \boldsymbol{\theta} + \mathbf{d})^\top \mathbf{p} + \boldsymbol{\lambda}^\top (\mathbf{A} \mathbf{p} - \mathbf{E} \boldsymbol{\theta} - \mathbf{b}) + \boldsymbol{\mu}^\top (\mathbf{B} \mathbf{p} - \mathbf{F} \boldsymbol{\theta} - \mathbf{y}). \quad (10)$$

Assume (9) is solved for  $\boldsymbol{\theta}_o \in \Theta$  and let  $(\mathbf{p}_o; \boldsymbol{\lambda}_o, \boldsymbol{\mu}_o)$  be the obtained optimal primal/dual solutions. Let also  $\mathbf{A}$  be the submatrix obtained from  $\mathbf{A}$  upon selecting the rows

corresponding to the active constraints in (9b). The remaining rows of  $\mathbf{A}$  related to *inactive constraints*, that is constraints satisfied with strict inequality, constitute matrix  $\bar{\mathbf{A}}_o$ . Similar partitions yield  $(\tilde{\mathbf{E}}, \tilde{\mathbf{b}}, \tilde{\boldsymbol{\lambda}})$  and  $(\bar{\mathbf{E}}, \bar{\mathbf{b}}, \bar{\boldsymbol{\lambda}})$ . The Karush-Kuhn-Tucker conditions for (9) provide

$$\mathbf{H} \mathbf{p}_o + \mathbf{C} \boldsymbol{\theta} + \mathbf{d} + \tilde{\mathbf{A}}^\top \tilde{\boldsymbol{\lambda}}_o + \mathbf{B}^\top \boldsymbol{\mu}_o = \mathbf{0} \quad (11a)$$

$$\tilde{\mathbf{A}} \mathbf{p}_o = \tilde{\mathbf{E}} \boldsymbol{\theta} + \tilde{\mathbf{b}} \quad (11b)$$

$$\mathbf{B} \mathbf{p}_o = \mathbf{F} \boldsymbol{\theta} + \mathbf{y} \quad (11c)$$

$$\bar{\mathbf{A}} \mathbf{p}_o < \bar{\mathbf{E}} \boldsymbol{\theta} + \bar{\mathbf{b}} \quad (11d)$$

$$\tilde{\boldsymbol{\lambda}}_o \geq \mathbf{0} \quad (11e)$$

$$\bar{\boldsymbol{\lambda}}_o = \mathbf{0}. \quad (11f)$$

We next consider separately the cases where (9) is: *a*) a strictly convex MPQP ( $\mathbf{H} \succ \mathbf{0}$ ) and *b*) an MPLP  $\mathbf{H} = \mathbf{0}$ . For both cases, it is further assumed that matrix

$$\mathbf{K} := [\tilde{\mathbf{A}}^\top \quad \mathbf{B}^\top]^\top \quad (12)$$

is full row-rank. This condition is known as *linearly independent constraint qualification (LICQ)*. Although LICQ cannot be guaranteed before solving (9) for a  $\boldsymbol{\theta}$ , it occurs in the majority of our tests in Section VI.

Commencing with  $\mathbf{H} \succ \mathbf{0}$  and under LICQ, the system of linear equations formed by (11a)–(11c) has a unique solution, and the primal/dual solutions of (9) can be obtained as

$$\begin{bmatrix} \mathbf{p}_o \\ \tilde{\boldsymbol{\lambda}}_o \\ \boldsymbol{\mu}_o \end{bmatrix} = \mathbf{M} \boldsymbol{\theta}_o + \mathbf{r} = \begin{bmatrix} \mathbf{M}_1 \\ \mathbf{M}_2 \\ \mathbf{M}_3 \end{bmatrix} \boldsymbol{\theta}_o + \begin{bmatrix} \mathbf{r}_1 \\ \mathbf{r}_2 \\ \mathbf{r}_3 \end{bmatrix} \quad (13)$$

where

$$\mathbf{M} = \begin{bmatrix} \mathbf{M}_1 \\ \mathbf{M}_2 \\ \mathbf{M}_3 \end{bmatrix} := \begin{bmatrix} \mathbf{H} & \tilde{\mathbf{A}}^\top & \mathbf{B}^\top \\ \tilde{\mathbf{A}} & \mathbf{0} & \mathbf{0} \\ \mathbf{B} & \mathbf{0} & \mathbf{0} \end{bmatrix}^{-1} \begin{bmatrix} -\mathbf{C} \\ \tilde{\mathbf{E}} \\ \mathbf{F} \end{bmatrix} \quad (14a)$$

$$\mathbf{r} = \begin{bmatrix} \mathbf{r}_1 \\ \mathbf{r}_2 \\ \mathbf{r}_3 \end{bmatrix} := \begin{bmatrix} \mathbf{H} & \tilde{\mathbf{A}}^\top & \mathbf{B}^\top \\ \tilde{\mathbf{A}} & \mathbf{0} & \mathbf{0} \\ \mathbf{B} & \mathbf{0} & \mathbf{0} \end{bmatrix}^{-1} \begin{bmatrix} \mathbf{d} \\ \tilde{\mathbf{b}} \\ \mathbf{y} \end{bmatrix}. \quad (14b)$$

The matrix inverse in (14a)–(14b) exists, since its determinant equals  $\det(\mathbf{H}) \det(-\mathbf{K} \mathbf{H}^{-1} \mathbf{K}^\top) < 0$  from Schur's complement. If (9) is an MPLP, suppose further that  $\mathbf{K}$  is square. This holds if in addition to LICQ, the number of active constraints equals the number of optimization variables.

Upon rearranging (11), the primal/dual solutions of (9) take again the closed-form expression of (13), but with

$$\mathbf{M}_1 := \mathbf{K}^{-1} \begin{bmatrix} \tilde{\mathbf{E}} \\ \mathbf{F} \end{bmatrix} \quad \text{and} \quad \mathbf{r}_1 := \mathbf{K}^{-1} \begin{bmatrix} \tilde{\mathbf{b}} \\ \mathbf{y} \end{bmatrix} \quad (15a)$$

$$\begin{bmatrix} \mathbf{M}_2 \\ \mathbf{M}_3 \end{bmatrix} := \mathbf{K}^{-\top} \mathbf{C} \quad \text{and} \quad \begin{bmatrix} \mathbf{r}_2 \\ \mathbf{r}_3 \end{bmatrix} := \mathbf{K}^{-\top} \mathbf{d}. \quad (15b)$$

One of the interesting claims of MPLP/MPQPs is that for any other  $\boldsymbol{\theta} \in \Theta$  yielding rise to the same set of active constraints, the primal/dual solutions are expressed through (13); see e.g., [7], [8]. Contrarily, given a set of constraints, the subset of  $\boldsymbol{\theta}$ 's activating those constraints can be identified as a polytope  $\mathcal{C} \subseteq \Theta$  described as [8]

$$\mathcal{C} := \{ \boldsymbol{\theta} \in \Theta \mid (\bar{\mathbf{A}} \mathbf{M}_1 - \bar{\mathbf{E}}) \boldsymbol{\theta} \leq \bar{\mathbf{b}} - \bar{\mathbf{A}} \mathbf{r}_1, \mathbf{M}_2 \boldsymbol{\theta} \geq \mathbf{r}_2 \} \quad (16)$$

that is derived from the primal/dual feasibility conditions of (11d)–(11e). The quantities  $(\mathbf{M}_1, \mathbf{M}_2, \mathbf{r}_1, \mathbf{r}_2)$  are provided by (14) or (15) for MPQP and MPLP, accordingly. The set  $\mathcal{C}$  is termed a *critical region* of  $\Theta$ . We next leverage these MPP properties to cope with (4) in two different ways.

## V. STRATEGIC INVESTMENT VIA MPP

To derive efficient solvers for the strategic investment task of (4), the key idea is to cast the inner problem as a multiparametric program and exploit the rich properties for its solutions. If the bidding functions in (1) are quadratic or (piecewise) affine, then (1) is an instance of (9). The optimization variable  $\mathbf{p}$  stacks the variables  $(\mathbf{p}_r, \mathbf{p}_e, \mathbf{p}_n)$ . The parametric inequalities of (9b) capture the line flow constraints of (1c) and the generation limits of (1d)–(1e). The parametric equalities (9c) relate to the power balance constraint of (1b).

The parameter  $\theta$  consists of three parts. The first part relates to the uncertainties in the cost coefficients (changing bids). This is reflected by the second summand in (9a), under the assumption that the quadratic component  $\frac{1}{2}\mathbf{p}^\top \mathbf{H}\mathbf{p}$  remains invariant (if present) across scenarios. The second part of  $\theta$  captures the uncertain demand vector  $\ell$ . The third part models changing unit capacities, including the units under investment. In summary, the parameter vector can be expressed as  $\theta := [\mathbf{c}^\top \ \ell^\top \ \bar{\mathbf{p}}^\top]^\top$ , where  $\mathbf{c} := [\mathbf{c}_r^\top \ \mathbf{c}_e^\top \ \mathbf{c}_n^\top]^\top$  and  $\bar{\mathbf{p}} := [\bar{\mathbf{p}}_r^\top \ \bar{\mathbf{p}}_e^\top \ \bar{\mathbf{p}}_n^\top]^\top$ . To map the cost of (9) to the one in (1), set  $\mathbf{C} = [\mathbf{I} \ \mathbf{0} \ \mathbf{0}]$  and  $\mathbf{d} = \mathbf{0}$ . The mappings related to the constraints are straightforward and are not presented here.

It is worth mentioning here that the parameter  $\theta$  of (1) depends on the variable  $\mathbf{x}$  of the outer layer in (4), as well as the *uncertain quantities* collectively denoted by  $\omega$ , namely the bids, loads, rival and existing unit capacities, capacity factors for new units. Due to the multiplication  $\bar{\mathbf{p}}_n = \alpha \odot \mathbf{x}$ , the mapping from  $(\omega, \mathbf{x})$  to  $\theta$  is nonlinear and will be abstractly denoted by  $\theta = \mathcal{P}(\omega, \mathbf{x})$ . Despite  $\mathcal{P}$  being nonlinear, problem (1) remains linear in  $\theta$ , so the MPP theory is applicable. Having posed (1) as an instance of (9), we next present two methods that leverage the affine mappings of (13)–(15) and the partitioning of (16) to solve (7).

### A. An MPP-aided Grid Search (MPP-GS) Scheme

This section exploits the MPP toolbox of Section IV to efficiently solve (1) for a large number of  $(\omega, \mathbf{x})$  instances. We can thus evaluate  $\hat{f}(\mathbf{x})$  over a grid of  $\mathbf{x}$  values in an efficient manner. This grid search approach is preferred when an investor is presented with a single or few possible investment locations, so that the optimization vector  $\mathbf{x}$  has several of its entries zeroed beforehand. To design our search grid, note first that the investment  $x_m$  at bus  $m$  can be bounded as

$$\bar{x}_m = \sum_{a:(m,k)} \bar{f}_a + \sum_{a:(k,m)} \bar{f}_a + \max_t \{\ell_{m,t}\} \quad (17)$$

by the maximum load at bus  $m$  plus the sum of capacities for all transmission lines incident to bus  $m$ . The quantity  $\bar{x}_m$  is the maximum power that can be produced at bus  $m$  without violating any physical limits. The discretization step over  $[0, \bar{x}_m]$  can be chosen based on the type of the power

---

### Algorithm 1 MPP-aided Grid Search (MPP-GS)

---

**Input:** Set of OPF scenarios  $\hat{\Theta} = \{\theta_s\}_{s=1}^{KT}$   
**Output:** OPF solutions  $\{\pi_s, \mathbf{p}_{e,s}, \mathbf{p}_{n,s}\}_{s=1}^{KT}$  to (1) via (9) for all  $\theta_s \in \hat{\Theta}$

- 1: **while**  $\hat{\Theta} \neq \emptyset$  **do**
- 2: Randomly select  $\theta_o \in \hat{\Theta}$  and  $\hat{\Theta} \leftarrow \hat{\Theta} \setminus \theta_o$
- 3: Solve (9) for  $\theta_o$  to find its primal/dual solutions and active constraints
- 4: Record  $(\mathbf{p}_{e,o}, \mathbf{p}_{n,o}, \pi_o)$
- 5: **if** matrix  $\mathbf{K}$  of (12) is full row-rank, **then**
- 6: Compute region's parameters  $(\mathbf{M}, \mathbf{r})$  from (13)
- 7: Compute region's polytope  $\mathcal{C}$  from (16)
- 8: **for all**  $\theta_s \in \hat{\Theta}$  **do**
- 9: **if**  $\theta_s \in \mathcal{C}$  [satisfying (16)], **then**
- 10: Compute OPF solution as  $\mathbf{p}_s = \mathbf{M}\theta_s + \mathbf{r}$
- 11: Record  $(\mathbf{p}_{e,s}, \mathbf{p}_{n,s}, \pi_s)$
- 12:  $\hat{\Theta} \leftarrow \hat{\Theta} \setminus \theta_s$
- 13: **end if**
- 14: **end for**
- 15: **end if**
- 16: **end while**
- 17: Evaluate  $\hat{f}(\mathbf{x})$  over  $\hat{\mathcal{X}}$  and find the minimizing  $\mathbf{x}$

---

plant. For example, a typical wind turbine is about 2-3 MW, so that multiples of this value are reasonable options for the grid step. When investing at  $M$  locations with  $K_m$  search values per location  $m$ , we get a search grid  $\hat{\mathcal{X}} \subseteq \mathcal{X}$  of  $K = \prod_{m=1}^M K_m$  points. Since  $K$  grows exponentially with  $M$ , this approach makes sense only for  $M = 1 - 3$  locations.

Given the search grid  $\hat{\mathcal{X}}$  and the uncertain parameter set  $\Omega := \{\omega_t\}_{t=1}^T$ , one can readily form the parameter set  $\hat{\Theta}$  using the mapping  $\mathcal{P} : \hat{\mathcal{X}} \times \Omega \rightarrow \hat{\Theta}$  and  $|\hat{\Theta}| = KT$ . Here  $\hat{\Theta}$  is a finite subset of  $\Theta$ , over which (9) has to be solved. This slightly abuses notation since in Section IV symbol  $\Theta$  denoted the convex set of  $\theta$ 's rendering (9) feasible. A solution to (7) can be found by solving (1) in its parameterized form of (9) for all  $KT$  members of  $\hat{\Theta}$ , and then evaluating  $\hat{f}(\mathbf{x})$  over  $\hat{\mathcal{X}}$ . For  $\hat{f}(\mathbf{x})$  to be a reasonable estimate of  $f(\mathbf{x})$  though, a large number  $T$  of scenarios  $\omega_t$  needs to be considered, yielding a computationally formidable task even for small  $K$ .

Thanks to MPP however, problem (9) needs to be solved for just as many times as the critical regions appearing in  $\hat{\Theta}$ . To see this, suppose that for a critical region  $\mathcal{C}_o \subseteq \Theta$ , we have already computed its polytopical description in (16) and the pair  $(\mathbf{M}, \mathbf{r})$  parameterizing its primal/dual solutions. Then, for any other  $\theta_s \in \hat{\Theta}$  belonging to  $\mathcal{C}_o$ , we can directly compute its primal/dual solutions from (13) without having to solve (9). This procedure, termed *MPP-based Grid Search (MPP-GS)*, is formalized as Algorithm 1 and its steps are explained next.

MPP-GS selects a  $\theta_o$  from  $\hat{\Theta}$  at step 2. At step 3, it solves (9) for  $\theta_o$ . If the related  $\mathbf{K}$  is of full row rank, the algorithm constructs a description for the visited critical region (steps 6-7). It further scans the remaining dataset  $\hat{\Theta}$  to find other  $\theta_s$ 's belonging to this region (step 8); computes their solution in closed form (steps 10-11); and removes these  $\theta_s$ 's from  $\hat{\Theta}$  (step 12). The process continues until  $\hat{\Theta}$  becomes empty.

MPP-GS explores a critical region only when  $\mathbf{K}$  is of full row rank (step 5). Albeit such cases could be potentially handled [7], [8], they involve methods of high complexity. Instead, when we come across a such instance of (9), we only record its primal/dual solutions. During the tests of Section VI, these instances appear infrequently. Vectors  $\theta_s$  are visited in an arbitrary rather than sequential fashion, by randomly sampling from  $\hat{\Theta}$  (step 2). In this way, we increase the chances of exploring more popular critical regions early on. It is hence more likely to handle a larger number of  $\theta_s$ 's earlier, so that  $\hat{\Theta}$  shrinks faster and step 9 is run on progressively much fewer  $\theta_s$ 's. To cope with (7) for larger  $K$  or  $T$ , we next pursue an MPP-aided stochastic gradient descent approach.

### B. MPP-aided Stochastic Gradient Descent (MPP-SGD)

The objective  $\hat{f}(\mathbf{x})$  of (7) involves a summation over a large number  $T$  of scenarios  $\omega_t$ . Rather than finding the costly gradient of  $\hat{f}(\mathbf{x})$ , we adopt stochastic approximation and update  $\mathbf{x}$  by taking each time a descent step over the gradient for only one of the summands of  $\hat{f}(\mathbf{x})$ . Define the summand of  $\hat{f}(\mathbf{x})$  related to scenario  $\omega_t$  as

$$f_t(\mathbf{x}) := \mathbf{k}^\top \mathbf{x} - \boldsymbol{\pi}_t^\top (\mathbf{p}_{e,t} + \mathbf{p}_{n,t}) + g_e(\mathbf{p}_{e,t}) + g_n(\mathbf{p}_{n,t}). \quad (18)$$

Recall the dispatches  $(\mathbf{p}_{e,t}, \mathbf{p}_{n,t})$  and prices  $\boldsymbol{\pi}_t$  are all functions of  $\mathbf{x}$ , since they are outcomes of (1) given  $\mathbf{x}$ .

Apparently  $\nabla_{\mathbf{x}}(\mathbf{k}^\top \mathbf{x}) = \mathbf{k}$ . To study the differentiability of the remaining terms of  $f_t$ , assume for now that  $\theta = \mathcal{P}(\omega_t, \mathbf{x})$  is strictly inside a critical region  $\mathcal{C}_o \subseteq \Theta$ . According to (13), the optimal dispatch vectors  $\mathbf{p}_{e,t}$  and  $\mathbf{p}_{n,t}$  are affine functions of  $\theta$ . Therefore, these vectors are affine functions of  $\mathbf{x}$  for a particular  $\omega_t$ . Appealing to (2), the optimal prices  $\boldsymbol{\pi}_t$  are linear functions of  $(\boldsymbol{\lambda}, \boldsymbol{\mu})$ . Since  $(\boldsymbol{\lambda}, \boldsymbol{\mu})$  are affine functions of  $\theta$  from (13), the prices  $\boldsymbol{\pi}_t$  are affine functions of  $\theta$  too. Consequently, the revenue term  $\boldsymbol{\pi}_t^\top (\mathbf{p}_{e,t} + \mathbf{p}_{n,t})$  is quadratic in  $\mathbf{x}$  and its gradient is of the form

$$\nabla_{\mathbf{x}} [\boldsymbol{\pi}_t^\top (\mathbf{p}_{e,t} + \mathbf{p}_{n,t})] = \mathbf{Q}_o \theta + \mathbf{q}_o. \quad (19)$$

The parameters  $(\mathbf{Q}_o, \mathbf{q}_o)$  can be computed using (13). Heed these parameters remain constant within each critical region of  $\Theta$ , that is for all pairs  $(\omega_t, \mathbf{x})$  for which  $\theta = \mathcal{P}(\omega_t, \mathbf{x}) \in \mathcal{C}_o$ . As in Section V-A, the uncertain parameters  $\omega_t$  are drawn from a finite set of scenarios. On the contrary, the investment variable  $\mathbf{x}$  is drawn now from a continuous set.

Regarding the term  $g_e(\mathbf{p}_{e,t}) + g_n(\mathbf{p}_{n,t})$ , its gradient with respect to  $\mathbf{x}$  can be computed using the chain rule, since functions  $(g_e, g_n)$  are known (quadratic or affine) and  $(\mathbf{p}_{e,t}, \mathbf{p}_{n,t})$  are affine functions of  $\theta$  and consequently  $\mathbf{x}$ .

Consider now the case where  $\theta = \mathcal{P}(\omega_t, \mathbf{x})$  is on a boundary between critical regions. Then, functions  $\boldsymbol{\pi}_t^\top (\mathbf{p}_{e,t} + \mathbf{p}_{n,t})$ ,  $g_e(\mathbf{p}_{e,t})$ , and  $g_n(\mathbf{p}_{n,t})$  may not be differentiable or even continuous in  $\mathbf{x}$ . Take for example the 3-bus example of Section II-C. Figure 3 plots function  $\pi_1 p_1$  over  $\theta = \mathcal{P}(\ell_3, x_1) = [\ell_3 \ x_1]^\top$  along with the related critical regions. Evidently, the function is differentiable within each region, but not on their boundaries. Nonetheless, these boundaries are zero-probability events over  $\Theta$ . Being a stochastic algorithm, the probability of coming across such  $\theta$ 's during the SGD iterations is zero.

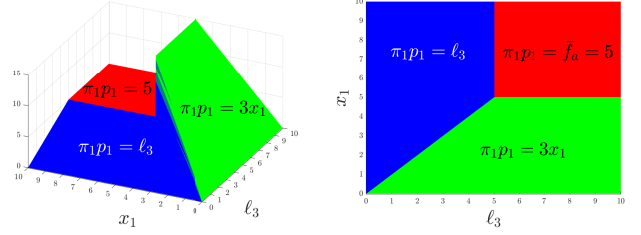


Fig. 3. *Left:* The function  $\pi_1 p_1$  for the example of Fig. 1 for  $x_1 \in [0, 10]$  and  $\bar{f}_a = 5$ . Due to the linear bidding functions and zero generation cost, the product  $\pi_1 p_1$  becomes an affine or constant function of  $\theta = [\ell_3, x_1]^\top$  rather than quadratic. *Right:* The blue critical region of  $\theta$  corresponds to  $p_2$  hitting its lower limit ( $p_2 = 0$ ); the green region to  $p_1$  hitting its upper limit  $p_1 = x_1$ ; and the red region to line  $(1, 3)$  being congested.

Instead of updating  $\mathbf{x}$  for one  $\omega_t$  at a time, we exploit the MPP toolbox and derive a mini-batch rendition to get improved algorithmic convergence at a minimal increase of computational complexity. The key idea is because of the MPP results, we can compute gradients efficiently with respect to  $\mathbf{x}$  not for a single  $\omega_t$ , but possibly for multiple  $\omega_t$ 's at a time. To elaborate, notice that for a particular  $\mathbf{x}_o$ , all  $\theta_t = \mathcal{P}(\omega_t, \mathbf{x}_o)$  that belong to the same critical region share the same gradient coefficients  $(\mathbf{Q}_o, \mathbf{q}_o)$  according to (19). Hence, all these gradients can be readily computed once this critical region, its parameters  $(\mathbf{M}, \mathbf{r})$ , and its polytopic description of (16) have been identified.

Our MPP-aided stochastic gradient descent algorithm is tabulated as Algorithm 2. Step 3 constructs a parameter set  $\Theta^k$  based on the current estimate of the investment vector  $\mathbf{x}^k$  and all scenarios  $\omega_t$ 's. In steps 4-8, a random  $\theta_o$  is drawn from  $\Theta^k$  and we identify the region it belongs to. Steps 9-14 compute the gradient with respect to  $\mathbf{x}$  for all  $\theta \in \Theta^k$  and sum them up in  $\mathbf{g}^k$ . Step 12 counts the members of the said region, so that we can compute the average gradient in step 16. The updates of step 17 are guaranteed to converge to a stationary point [17]. The random draw of step 4 ensures an unbiased exploration of regions in  $\Theta$ , hence the average gradient per region is an unbiased estimate of the gradient of  $f(\mathbf{x})$  in (7).

## VI. NUMERICAL TESTS

All tests were run on the IEEE 118-bus system with 54 generators and 186 lines [18]. Line limits were estimated from surge impedances as explained in [19]. We used bidding and load data from PJM for 2018. This dataset has only 21 load profiles. To obtain a load profile for each of the 118 buses, one of the base load profiles was selected at random and perturbed by  $\pm 5\%$  with zero-mean Gaussian noise, and scaled so its annual maximum matched the benchmark nominal load.

Regarding generation costs, for all thermal units the actual generation cost matched the market bid or  $f_e(\mathbf{p}_{e,t}) = g_e(\mathbf{p}_{e,t})$ . For wind units, the actual generation cost as well as their bid into the market is assumed to be zero. We assumed wind turbines with  $3 \times 10^6$  \$/MW investment cost with a life span of 25 years and an additional  $4 \times 10^4$  \$/MW for operation and maintenance costs, yielding  $k = 1, 826.5$  assuming a base apparent power of 100 MVA.

**Algorithm 2** MPP-Stochastic Gradient Descent (MPP-SGD)

**Input:**  $\Omega$ , initialization  $\mathbf{x}_o$ , tolerance  $\tau$ , and step size  $\eta$ 
**Output:** Optimal investment  $\mathbf{x}^*$ 

- 1: Set  $\mathbf{x}^0 = \mathbf{x}_o$ ,  $\epsilon > \tau$ ,  $k = 0$
- 2: **while**  $\epsilon \geq \tau$  **do**
- 3: Define  $\Theta^k \leftarrow \{\theta_1^k, \dots, \theta_T^k\}$  where  $\theta_t^k = \mathcal{P}(\omega_t, \mathbf{x}^k)$
- 4: Randomly select  $\theta_o$  from  $\Theta^k$
- 5: Solve (9) for  $\theta_o$  to find its primal/dual solutions and active constraints
- 6: Set  $\mathbf{g}^k \leftarrow \mathbf{0}$  and  $c^k \leftarrow 0$
- 7: **if** matrix  $\mathbf{K}$  is full row-rank, **then**
- 8: Compute region's parameters  $(\mathbf{M}, \mathbf{r})$  from (13) and gradient coefficients  $(\mathbf{Q}, \mathbf{q})$
- 9: Compute region's polytope  $\mathcal{C}$  from (16)
- 10: **for** all  $\theta_t^k \in \Theta^k$  **do**
- 11: **if**  $\theta_t^k \in \mathcal{C}$ , **then**
- 12: compute the gradient  $\mathbf{g}_t$  and set  $\mathbf{g}^k \leftarrow \mathbf{g}^k + \mathbf{g}_t$
- 13: set  $c^k \leftarrow c^k + 1$
- 14: **end if**
- 15: **end for**
- 16: **end if**
- 17: Set  $\mathbf{x}^{k+1} \leftarrow \left[ \mathbf{x}^k - \frac{\eta}{c^k \sqrt{k}} \mathbf{g}^k \right]_{\mathcal{X}}$
- 18: Compute the moving average  $\bar{\mathbf{x}}^k \leftarrow \frac{\sum_{i=\lceil k/2 \rceil}^k (\mathbf{x}^{(i)}/\sqrt{i})}{\sum_{i=\lceil k/2 \rceil}^k \sqrt{i}}$
- 19: Set  $\epsilon \leftarrow \frac{\|\bar{\mathbf{x}}^k - \bar{\mathbf{x}}^{(k-1)}\|}{\|\bar{\mathbf{x}}^k\|}$  and  $k \leftarrow k + 1$
- 20: **end while**
- 21: Set  $\mathbf{x}^* = \bar{\mathbf{x}}^k$

All tests were performed on a computer with Intel Core i7 @ 3.4 GHz (16 GB RAM). Problem (9) was solved using the ECOS solver in YALMIP [20], [21]. For our MPP algorithms, we need to identify active constraints, so we can compute the quantities in (13)–(16). To the best of our knowledge, ECOS or any other QP solver does not identify active constraints explicitly. Because of this, we declared a constraint as active if and only if the corresponding entry of the constraint satisfaction vector  $\mathbf{A}\mathbf{p} - \mathbf{E}\boldsymbol{\theta} - \mathbf{b}$  at the optimum was less than  $10^{-4}$ . This test may not classify correctly a constraint as active or not. To alleviate such errors, we also checked whether  $\theta_o$  belongs to its own region (the region identified by solving (9) for  $\theta_o$ ) with an accuracy of  $10^{-5}$ . We recorded the region only if this second test was successful. Otherwise, we recorded only the primal/dual solutions for that  $\theta_o$ .

In the first test, we considered investing on a wind farm at 4 different single locations. Existing units were hosted at buses 1, 4, and 6 for all investing scenarios. For the new unit, we considered buses 117 and 29 that are relatively electrically close to the existing units, and buses 67 and 95 that are far, to show the effect of new units on existing units. We tested three wind capacity factors; two obtained from [22] for 2018 scaled to have a mean of  $\mu_\alpha = 0.5$  and  $\mu_\alpha = 0.75$ ; and one with no randomness ( $\mu_\alpha = 1$ ). For each single location ( $M = 1$ ), we considered  $K = 10$  investment values hourly over a year ( $T = 8,760$ ), yielding a total of 87,600 instances of (9). Figure 4 depicts the average total cost  $\hat{f}(x)$  and the average cost for new units defined as  $\hat{f}_n(x) := \frac{1}{T} \sum_{t=1}^T -\boldsymbol{\pi}_t^\top \mathbf{p}_n$ .

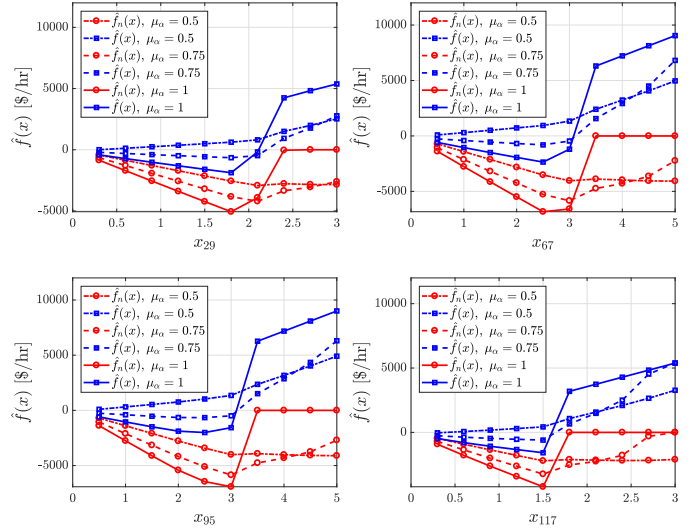


Fig. 4. Total and new unit costs  $\hat{f}(x)$  and  $\hat{f}_n(x)$  for buses 29, 67, 95, and 117 for wind capacity factors with mean  $\mu_\alpha = \{0.5, 0.75, 1\}$ .

TABLE I  
TOTAL COMPUTATION TIME [H] PER BUS AND WIND CAPACITY

Bus	$\mu_\alpha = 0.5$	$\mu_\alpha = 0.75$	$\mu_\alpha = 1$
29	0.44	0.55	0.65
67	0.57	1.12	1.66
95	0.62	1.33	1.63
117	0.57	1.08	1.31

Table II shows the running times for the first two tests of MPP-GS. For comparison, we randomly drew 1,000  $\theta$ 's and recorded the run-times for solving (9) without using MPP. This test resulted in an average running time of 0.32 sec with a standard deviation of 0.224 sec. These running times mean that solving 87,600 scenarios would take an average of 7.8 hours.

The first observation is that having higher wind capacity factors, the total cost is lower as expected. Interestingly, these results also show that the cost  $\hat{f}_n(x)$  for new units increases after  $x$  exceeds some value, so with more investment the revenue decreases. This counter-intuitive reduction in revenue is because these units have zero marginal cost and hence, larger capacity  $x$  incurs higher chances of being a marginal generator resulting in zero price at the same bus.

In the second test, we tested MPP-SGD for investing at the single locations of the previous test with wind capacity factors of  $\mu_\alpha = 0.75$  and  $\mu_\alpha = 1$ . We chose a step size of  $\eta = 10^{-4}$  and tolerance  $\tau = 10^{-8}$ . Figure 5 illustrates the moving average  $\bar{x}$  for each bus and for four different initializations. These results demonstrate the robustness of MPP-SGD to initialization and locations. Table II reports the running times for  $\mu_\alpha = 0.75$ .

In the third test, MPP-SGD was applied for SI at multiple locations. Figure 5 demonstrates the moving average  $\bar{x}$  for investing at 2, 4, 8, and 16 locations. The total invested capacity was upper bounded by 300 MW to study the effect of a coupling constraint in  $\mathcal{X}$ . The lower bound for investment was also set to  $10^{-3}$  to remove the possibility of trivial active

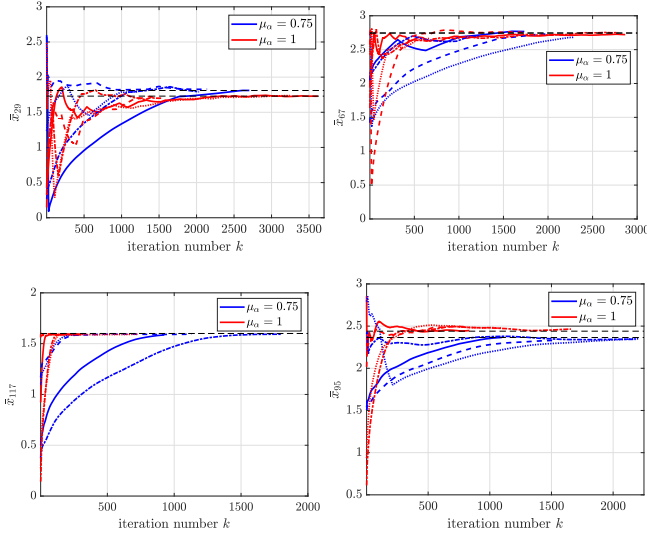


Fig. 5. The sliding average  $\hat{x}$  computed by MPP-SGD randomly initialized at  $x^{(0)} \in [0, \hat{x}]$  for buses 29, 67, 95, and 117 (clockwise).

TABLE II  
TOTAL COMPUTATION TIME [H] PER INITIALIZATION

Bus	$(x_0, \text{time})$	$(x_0, \text{time})$	$(x_0, \text{time})$	$(x_0, \text{time})$
29	(2.59, 0.77)	(2.57, 0.62)	(0.19, 0.44)	(1.23, 0.19)
67	(2.05, 0.35)	(1.42, 0.7)	(2.04, 0.26)	(2.71, 0.4)
95	(1.54, 0.29)	(1.51, 0.54)	(2.4, 0.7)	(2.79, 0.8)
117	(0.5, 0.3)	(1.16, 0.51)	(0.37, 0.25)	(1.11, 0.06)

constraints. Interestingly, the coupling constraint yielded a relatively sparse final investment.

## VII. CONCLUSIONS

We have uniquely exploited the properties of MPP to devise two SI solvers. The grid search algorithm can handle cases where the number of investment locations is low. Although the needed function evaluations constitute an enormous dataset of DC-OPF instances, their exact primal/dual solutions can be computed upon solving only a limited number of these OPFs, thus accelerating the search by 8-12 times. For larger numbers of investment locations, we have devised a stochastic gradient search scheme, which computes the gradient of the SI objective over entire critical regions in an extremely efficient manner. The developed tools facilitate faster and more educated energy market decisions, while the ideas put forth here can be proved fruitful for coping more efficiently with transmission expansion planning and contingency analysis.

## REFERENCES

- [1] D. Pozo, E. Sauma, and J. Contreras, "Basic theoretical foundations and insights on bilevel models and their applications to power systems," *Annals of Operations Research*, vol. 254, no. 1, pp. 303–334, Jul. 2017.
- [2] S. J. Kazempour, A. J. Conejo, and C. Ruiz, "Strategic generation investment using a complementarity approach," *IEEE Trans. Power Syst.*, vol. 26, no. 2, pp. 940–948, May 2011.
- [3] A. J. Conejo, L. B. Morales, S. J. Kazempour, and A. S. Siddiqui, *Investment in Electricity Generation and Transmission: Decision Making under Uncertainty*, 1st ed. Switzerland: Springer, 2016.
- [4] Y. Liu, R. Sioshansi, and A. J. Conejo, "Multistage stochastic investment planning with multiscale representation of uncertainties and decisions," *IEEE Trans. Power Syst.*, vol. 33, no. 1, pp. 781–791, Jan. 2018.

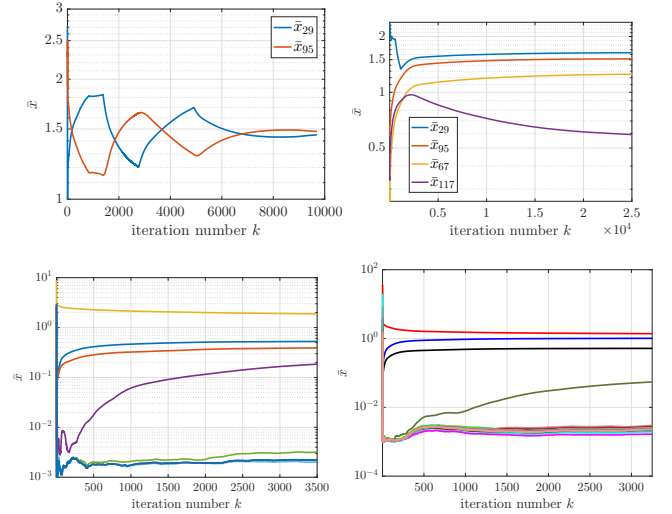


Fig. 6. MPP-SGD iterates for 2, 4, 8, and 16 investment locations.

- [5] F. D. Munoz and J.-P. Watson, "A scalable solution framework for stochastic transmission and generation planning problems," *Computational Management Science*, vol. 12, no. 4, pp. 491–518, Oct 2015.
- [6] V. Dvorkin, J. Kazempour, L. Baringo, and P. Pinson, "A consensus-ADMM approach for strategic generation investment in electricity markets," in *Proc. IEEE Conf. on Decision and Control*, Miami Beach, FL, USA, Dec. 2018, pp. 780–785.
- [7] F. Borrelli, A. Bemporad, and M. Morari, "Geometric algorithm for multiparametric linear programming," *Journal of Optimization Theory and Applications*, vol. 118, no. 3, pp. 515–540, Sep. 2003.
- [8] P. Tondel, T. A. Johansen, and A. Bemporad, "An algorithm for multi-parametric quadratic programming and explicit MPC solutions," *Automatica*, vol. 39, no. 3, pp. 489–497, 2003.
- [9] Q. Zhou, L. Tesfatsion, and C. Liu, "Short-term congestion forecasting in wholesale power markets," *IEEE Trans. Power Syst.*, vol. 26, no. 4, pp. 2185–2196, Nov. 2011.
- [10] Y. Ng, S. Misra, L. A. Roald, and S. Backhaus, "Statistical learning for DC optimal power flow," in *Proc. Power Systems Computation Conference*, Dublin, Ireland, Jun. 2018, pp. 1–7.
- [11] Y. N. Sidhant Misra, Line Roald, "Learning for constrained optimization: Identifying optimal active constraint sets," 2019. [Online]. Available: <https://arxiv.org/abs/1802.09639>
- [12] Y. Ji, R. J. Thomas, and L. Tong, "Probabilistic forecast of real-time LMP via multiparametric programming," in *International Conference on System Sciences*, Kauai, HI, USA, Jan. 2015, pp. 2549–2556.
- [13] X. Geng and L. Xie, "Learning the LMP-load coupling from data: A support-vector machine based approach," *IEEE Trans. Power Syst.*, vol. 32, no. 2, pp. 1127–1138, Mar. 2017.
- [14] S. Taheri, M. Jalali, V. Kekatos, and L. Tong, "Fast probabilistic hosting capacity analysis for active distribution systems," *IEEE Trans. Smart Grid*, 2020, (submitted). [Online]. Available: <https://arxiv.org/abs/2002.01980>
- [15] V. Kekatos, G. B. Giannakis, and R. Baldick, "Online energy price matrix factorization for power grid topology tracking," *IEEE Trans. Smart Grid*, vol. 7, no. 3, pp. 1239–1248, May 2016.
- [16] A. J. Wood and B. F. Wollenberg, *Power Generation, Operation, and Control*, 2nd ed. New York, NY: Wiley & Sons, 1996.
- [17] A. Nemirovski, A. Juditsky, G. Lan, and A. Shapiro, "Robust stochastic approximation approach to stochastic programming," *SIAM Journal on Optimization*, vol. 19, no. 4, pp. 1574–1609, 2009.
- [18] R. D. Zimmerman, C. E. Murillo-Sanchez, and R. J. Thomas, "MATPOWER: steady-state operations, planning and analysis tools for power systems research and education," *IEEE Trans. Power Syst.*, vol. 26, no. 1, pp. 12–19, Feb. 2011.
- [19] J. D. Glover, T. J. Overbye, and M. S. Sarma, *Power system analysis and design*, 6th ed. Boston, MA: Cengage Learning, 2017.
- [20] A. Domahidi, E. Chu, and S. Boyd, "ECOS: An SOCP solver for embedded systems," in *European Control Conference (ECC)*, Zurich, Switzerland, Jul. 2013, pp. 3071–3076.
- [21] J. Lofberg, "A toolbox for modeling and optimization in MATLAB,"

in *Proc. of the CACSD Conf.*, 2004. [Online]. Available: <http://users.isy.liu.se/johanl/yalmip/>

- [22] *Historical wind farm data*, Sotavento Galicia Foundation, accessed April 2018, <http://www.sotaventogalicia.com>.